Hepatic squamous cell carcinoma initially presenting as cholecystitis misdiagnosed as cholangiocarcinoma: A case report

GE SHI, XINHAN YE, FANGJIA YANG, ZHONG WANG and XIAOFENG MA

Department of Radiology, Zhuji People's Hospital, Zhuji, Zhejiang 311800, P.R. China

Received May 3, 2024; Accepted September 12, 2024

DOI: 10.3892/ol.2024.14749

Abstract. Primary squamous cell carcinoma of the liver (PSCCL) is a rare intrahepatic primary tumor. Due to a lack of distinctive clinical presentations and radiological features, early diagnosis is challenging. The present study, describes a patient who initially presented with symptoms indicative of cholecystitis but was misdiagnosed with cholangiocarcinoma. It is hypothesized that fluctuations in carcinoembryonic antigen levels during laboratory tests can significantly aid the diagnosis, treatment and prognosis of tumors. Furthermore, imaging studies are essential for the early diagnosis of PSCCL and the exclusion of metastatic squamous cell carcinoma.

Introduction

Primary squamous cell carcinoma of the liver (PSCCL) is an exceptionally rare and highly aggressive malignancy, with only a few cases reported worldwide (1), with <60 articles on primary hepatocellular carcinoma identified in the present comprehensive literature search from 1972 to 2024 (1). Unlike more common hepatic tumors, PSCCL lacks specific clinical and radiologic features, often leading to delay in diagnosis and treatment (2). Although the pathogenesis of PSCCL remains unclear, chronic liver disease and inflammatory responses are considered potential contributing factors (3). Due to its rarity, research into the therapeutic strategies for PSCCL primarily rely on case reports and small case series, with surgical resection being the most commonly employed intervention (4). However, the prognosis remains poor due to the high recurrence rate and limited efficacy of adjuvant therapies (5). It has been reported that only a limited number of patients survive beyond 12 months, even with treatment (1-11). Zhang *et al* (8) documented a median survival time of 7.5 months (range, 0.3 to 84 months) among 32 patients with available prognostic data (8). The present case report reviews the pathogenesis, clinical presentation, imaging characteristics and treatment outcomes of a patient with PSCCL, aiming to enhance the awareness of this rare tumor among clinicians and radiologists. The present report underscores the need for heightened suspicion of PSCCL in relevant clinical settings and imaging findings, with the goal of improving early diagnostic accuracy and optimizing patient outcomes.

Case report

The patient, a 64-year-old woman, came to the Department of Hepatobiliary Surgery of the People's Hospital of Zhuji (Zhuji, China) in October 2023, complaining of a right upper abdominal pain that had been persisting for two months, with no nausea or vomiting, and no chills or fever. Physical examination revealed the patient was alert and oriented, with no jaundice in the skin or mucous membranes, a soft and protuberant abdomen, tenderness in the upper abdomen without rebound pain, no palpable mass, and the liver and spleen not palpable below the ribs. The patient was negative for Murphy's sign and shifting dullness. The patient had no history of hepatitis infection, no surgical history, no family history of hereditary diseases and no other underlying diseases. Ultrasonography suggested the following: i) Heterogeneous echo mass near the gallbladder fossa in the right liver, with further examination recommended; ii) calcifications in the right liver; iii) rough gallbladder wall with multiple gallstones; and iv) enhanced pancreatic echogenicity. Abdominal CT scan and enhancement suggested (Fig. 1): i) Lesion near the gallbladder fossa in the right lobe of the liver, with magnetic resonance imaging (MRI) recommended for further examination; ii) multiple enlarged lymph nodes at the hepatic hilum; and iii) gallstones and cholecystitis. Liver MRI scan and enhancement suggested (Fig. 2): i) Occupying lesion in the right lobe of the liver with mild dilation of the intrahepatic bile ducts, suggesting the possibility of intrahepatic cholangiocarcinoma; and ii) gallstones and cholecystitis. Subsequent imaging studies failed to reveal any primary tumor.

Written informed consent was provided by the patient to obtain clinical data and information, as well as for publication. The present study included no personal information disclosure, and was approved by The Ethics Committee of Zhuji People's Hospital [Zhuji, China; approval no. (2024); MedEthics no. (0506)].

Correspondence to: Dr Xiaofeng Ma, Department of Radiology, Zhuji People's Hospital, 9 Ren'ai Road, Zhuji, Zhejiang 311800, P.R. China
E-mail: 649878980@qq.com

Key words: hepatic malignancy, squamous cell carcinoma, primary squamous cell carcinoma of the liver

Laboratory results. Blood samples were collected from the patient through venipuncture. Various hematological parameters were processed and analyzed using ELC electrochemiluminescence and IFCC (International Federation of Clinical Chemistry and Laboratory Medicine) methods. Tumor markers were detected using electrochemiluminescence, employing the fully automated Cobas e801 electrochemiluminescence immunoassay system [Roche Diagnostics (Shanghai) Ltd.]. Alanine aminotransferase (ALT) and aspartate aminotransferase (AST) were measured according to the IFCC method (12), while albumin (ALB) was assessed using the bromocresol green method (13), utilizing the fully automated BS-2800M biochemical analyzer (Shenzhen Mindray Bio-Medical Electronics Co., Ltd.). These data were derived from the patient's medical records. The laboratory results were as follows: α-Fetoprotein (AFP), 2.4 μg/l (reference values, 0.0-7.0 μg/l); carcinoembryonic antigen (CEA), 11.6 μg/l (reference values, 0.0-5.0 μg/l); cancer antigen 125 (CA-125), 32.3 KIU/l (reference values, 0.0-35.0 KIU/l); CA19-9, 228.0 KIU/l (reference values, 0.0-30.0 KIU/l); CA15-3, 11.2 KIU/l (reference values, 0.0-24.0 KIU/l); albumin, 35.3 g/l (reference values, 40.0-55.0 KIU/l); globulin, 26.4 g/l (reference values, 20.0-40.0 KIU/l); albumin/globulin ratio, 1.34 (reference values, 1.20-2.40); alanine transaminase, 7 U/l (reference values, 7-40 U/l); aspartate transferase, 8 U/l (reference values, 13-35 U/l); γ-glutamyl transferase, 43 U/l (reference values, 7-45 U/l); and white blood cells, 11.9x10^9/l (reference values, 3.5-9.5x10^9/l).

The patient presented with upper abdominal pain, tumor markers were elevated to varying degrees and there was no history of hepatitis or family history of tumors. Imaging studies revealed a liver mass, suggesting a malignant liver tumor. Based on the Barcelona Clinic Liver Cancer (BCLC) classification system (14), a preoperative assessment was conducted for the patient, evaluating tumor size, number, liver function, overall health status and the presence of extrahepatic metastasis. The patient exhibited normal liver and kidney function, with no distant metastases, and demonstrated adequate surgical tolerance. The patient was classified as BCLC A, making surgical resection the optimal treatment option. To prevent the ongoing inflammatory stimulation caused by gallstones, which could potentially lead to tumor recurrence, the patient exhibited normal liver and renal function, absence of distant metastasis and sufficient surgical tolerance. These factors enhanced the likelihood of surgical resection, and thus the patient met the criteria for surgical intervention.

The patient underwent a hepatic lobectomy and cholecystectomy at the People's Hospital of Zhuji (Zhuji, China) in October 2023. During the surgery, extensive adhesions were observed within the abdominal cavity, with severe adhesions between the right liver and the diaphragm. The liver texture was hard, with an uneven surface. Adhesions between the diaphragm and the liver surface were separated, revealing a tumor measuring ~6.5 cm in diameter located in the posterior lobe of the right liver. A biopsy specimen was first fixed using Zhejiang Jinhua Tonghe Biotechnology Co., Ltd. Biological Tissue Fixative (10% neutral buffered formalin fixative; ready-to-use) at 25˚C for 12 h, after which samples were cut to 3 μm-thick. The sections were stained with HE stain at 25˚C for 45 min and imaged using a Zeiss Axio-Lab-A1 microscope.

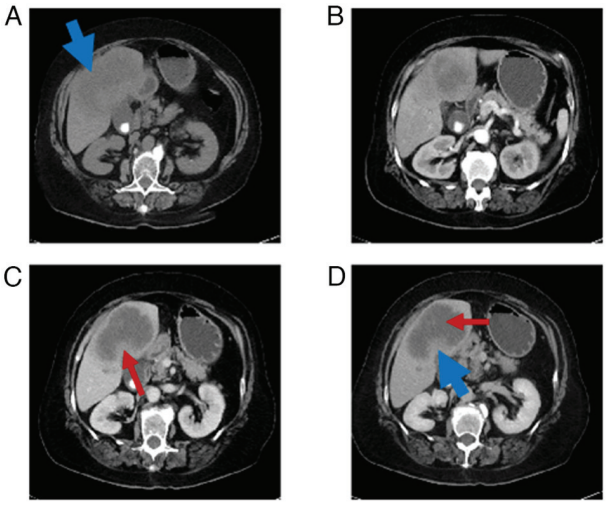

Figure 1. CT scan images of the patient. (A) Right lobe of the liver showed a slightly low-density shadow (thick arrow), uneven internal density and an unclear edge of the lesion. (B) In the arterial phase, there are focal and patchy areas of obvious enhancement at the periphery of the lesion. The inner wall is not smooth. No enhancement is observed in the central low-density area of the lesion. (C) In the portal venous phase, evident enhancement can still be observed in the lesion, and the solid enhancing component at the periphery of the lesion shows an increased range compared with the arterial phase (thin arrow), but no enhancement was found in the central low-density area. (D) In the delayed phase, the posterior part (thick arrow) of the lesion continued to intensify and the central low-density area was not enhanced (thin arrow).

Postoperative pathology revealed moderately differentiated squamous cell carcinoma of the right liver (measuring 12x6.5x6 cm), with the tumor infiltrating the full thickness of the gallbladder to the mucosa (Fig. 3A) and invading the muscular layer of the colon, while showing no invasion into omental tissue. Tumor tissue exhibited infiltrative growth, forming nests, pseudoadenoid structures and visible keratinized beads (Fig. 3B). The tumor cells were enlarged with significant atypia, abundant red cytoplasm, round nuclei, coarse chromatin, partial nucleoli and atypical nuclear division (Fig. 3C). The resection margins of the cystic duct and both sides of the colon were negative for tumor involvement. No definite tumor was observed in the stomach wall, liver or bile duct tissues. For immunohistochemistry, tissue sections (3-μm thick) were fixed in Zhejiang Jinhua Tonghe Biotechnology Co., Ltd., Biological Tissue Fixative (10% neutral buffered formalin) at 25˚C for 12 h, and embedded in paraffin. Staining was performed using the DAKO Autostainer Link 48 system (Agilent Technologies, Inc.). The following primary antibodies (prediluted by the manufacturer) from Guangzhou Anbiping Medical Laboratory Co., Ltd., were used: Ki67 (cat. no. IM098), CD10 (cat. no. IM025), EMA (cat. no. IR074), PAX-8 (cat. no. IR191), Vimentin (cat. no. IM142), CK7 (cat. no. IM061), CK (cat. no. IM067), CD34 (cat. no. IM034), P504s (cat. no. IR127), CK20 (cat. no. IR385), SMA (cat. no. IHC-M005), P53 (cat. no. IM123) and CD30 (cat. no. IM032). All primary antibodies were incubated with the samples at 25˚C for 30 min. The secondary antibodies EnVision FLEX+, Mouse, High pH (Link; prediluted by the manufacturer; cat. no. K8002; Agilent Technologies, Inc.; EnVision FLEX+) were used at 25˚C for 20 min. Blocking was performed with 3% peroxidase blocking reagent (cat. no. DAKO SM801; Agilent Technologies, Inc.)

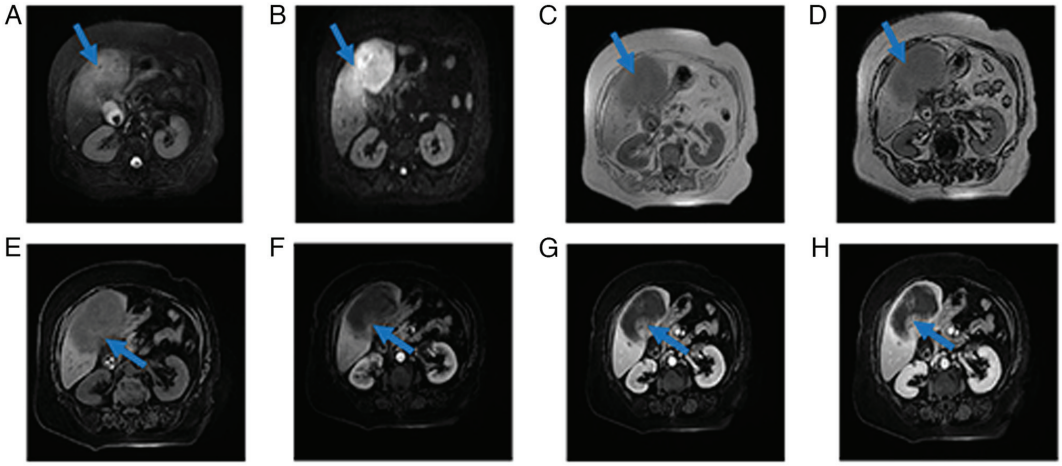

Figure 2. MRI scan images of the patient. (A) MRI T2WI sequence, a large mass in the right lobe of the liver can be seen, which is hyperintense, with uneven intern signals and unclear borders (blue arrow). (B) DWI sequence showed that the lesions showed obvious hyperintensity (blue arrow). (C) T1WI phase-inverse sequence, the lesion was hypointense (blue arrow), and (D) the reverse position was not reduced compared with the in-phase signal (blue arrow). (E) The right lobe of the liver is a large mass, and the LVAV sequence (blue arrow) shows that the lesion is hypointense and the margins are not clear. (F) Arterial phase scan showed mild enhancement of the edge of the lesion (blue arrow), no enhancement inside and the inner wall was not uniform. (G) Venous phase scan showed continuous enhancement at the edges of the lesion (blue arrow) and no enhancement internally. (H) The portal scan showed further enhancement at the edge of the lesion (blue arrow), and the extent was slightly larger than before, but the center was still not enhanced and had unclear borders. T1WI, T1-weighted imaging; T2WI, T2-weighted imaging; MRI, magnetic resonance imaging; DWI, diffusion weighted imaging; LVAV, liver vascular anatomy visualization.

at 25˚C for 5 min, followed by incubation with EnVision FLEX/HRP at 25˚C for 20 min. (cat. no. DAKO SM802; Agilent Technologies, Inc.). DAB incubation was carried out at 25˚C for 5 min (cat. no. DAKO DM827). The microscope used for examination was an Olympus BX-51 microscope with a camera adaptor (Olympus U-TV0.5XC-3; Olympus Corporation) for capturing images. Immunohistochemistry showed the following: P53 (wild type; data not shown), P63 (+; Fig. 3D), P40 (+; Fig. 3E), Ki-67 40% (+; data not shown), cytokeratin (CK)7 (+; data not shown), glypican-3 (-; data not shown), Her-2 (0; data not shown), HepPar1 (-; data not shown), AFP (-; data not shown), Arginase-1 (-; data not shown), CK19 (+; data not shown), CK20 (-; data not shown), CD34 (-; data not shown), SSTR2 (-; data not shown), CD56 (-; data not shown), Syn (-; data not shown), HSP 70 (+; data not shown) and GS (+; data not shown). Unfortunately, the patient declined treatment due to financial constraints and the high cost of chemotherapy and passed away in April 2024.

Following the collection and analysis of blood specimens, postoperative tumor marker reassessments provided the following results (Table I). A total of 40 days postoperatively, CEA and CA 19-9 levels returned to the normal range. However, during the 90-day follow-up, both markers showed an increase. By contrast, AFP remained within the normal range both preoperatively and postoperatively. After the observed increase in tumor marker levels, a comprehensive abdominal contrast CT scan was performed 100 days post-surgery (Fig. 4). A large occupying lesion in the surgical area, measuring ~12x8 cm was observed. The enhancement scan revealed rim and nodular enhancement at the periphery with no central enhancement.

Discussion

Pathological mechanism. PSCCL is an extremely rare hepatic malignancy, with only a handful of cases reported worldwide (1,6). The pathogenesis of PSCCL remains largely unclear. Studies suggest that PSCCL may be closely associated with chronic liver disease, inflammatory responses, intrahepatic epithelial metaplasia and squamous cell hyperplasia (2,4,6,7). Chronic liver conditions, such as cirrhosis and hepatitis B virus infection, can lead to prolonged chronic inflammation in hepatic cells (2,8). This persistent inflammatory state can activate multiple signaling pathways, triggering gene mutations and abnormal cell proliferation, thereby laying the groundwork for the development of PSCCL (1,4,8). As the chronic inflammation persists, normal intrahepatic glandular epithelial cells may undergo squamous metaplasia, a precursor for PSCCL formation (8). Additionally, PSCCL has been reported in association with hepatic cysts, intrahepatic stones, and, in rare instances, teratomas (9). In the case described in the present study, the patient initially presented with suspected cholecystitis, indicating a history of inflammation. Subsequent CT imaging revealed a hepatic mass, initially misdiagnosed as a liver abscess. However, upon further evaluation with imaging studies, tumor markers and immunohistochemical analysis, the final diagnosis of PSCCL was established. This case aligns with the proposed mechanisms of PSCCL pathogenesis.

Clinical presentation. The clinical manifestations of PSCCL are typically nonspecific and resemble those of other hepatic malignancies, making early diagnosis challenging (2,7). Most patients with PSCCL initially present with symptoms such as abdominal discomfort, fatigue, and weight loss (1,8). As the disease progresses, more pronounced signs may develop, including palpable liver masses (3,4,10). Rapid tumor growth may lead to right upper quadrant tenderness and abdominal distension (7,10). When the bile ducts are compressed or liver function is impaired, serum bilirubin and transaminase levels may be elevated, indicating that the disease has likely advanced to a late stage (10). Some patients may develop systemic symptoms, such as fever, particularly when the tumor

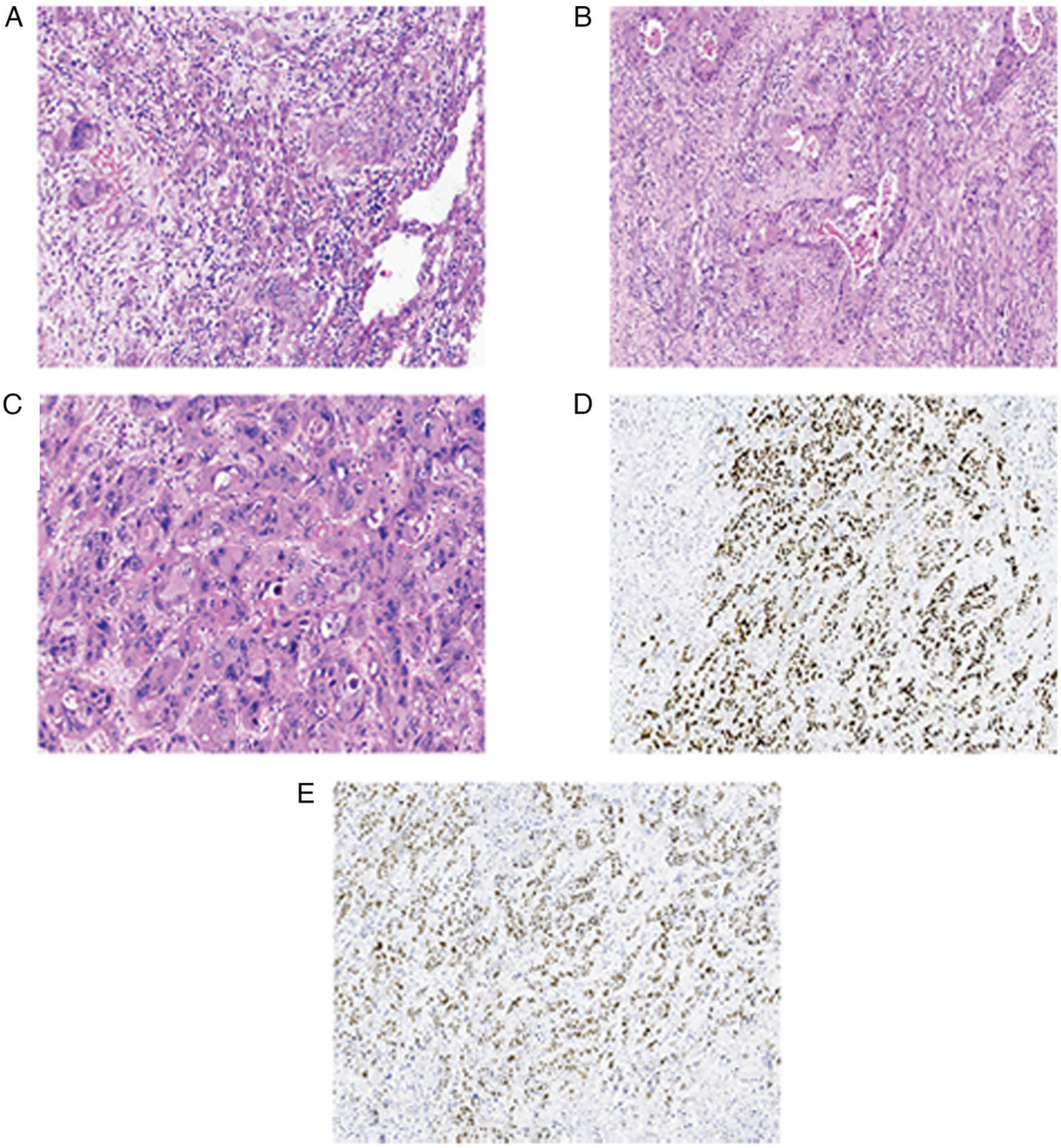

Figure 3. Postoperative pathological and immunohistochemical results of the patient. (A) Tumor tissue exhibited infiltrative growth, forming nests, pseudoadenoid structures (magnification, x200) and (B) visible keratinized beads (magnification, x100). (C) The tumor cells were enlarged with significant atypia, abundant red cytoplasm, round nuclei, coarse chromatin, partial nucleoli and atypical nuclear division (magnification, x200). (D) The presence of P63 was detected in the nucleus (magnification, x100). (E) The presence of P40 was detected in the nucleus (magnification, x100).

undergoes necrosis or secondary infection, occasionally leading to liver abscess formation (4). At present, no specific serum biomarkers for PSCCL have been identified, complicating the diagnostic process (2,4). In the present case, the patient exhibited significantly elevated levels of CA19-9 and CEA, which decreased following tumor resection. However, during follow-up, both markers rose again, and imaging studies suggested tumor recurrence, highlighting the potential importance of CA19-9 and CEA in the diagnosis and monitoring of PSCCL. Additionally, AFP levels in this patient did not show a significant increase, consistent with the findings of Zhao *et al* (1), who reported that AFP levels typically remain within normal ranges in PSCCL cases, whereas elevations in CEA, CA125 and CA19-9 are more common.

Imaging features. Due to the lack of specific clinical presentations and a poorly defined etiology, combined with the highly malignant and rapidly metastatic nature of PSCCL, early diagnosis is challenging (9). Although PSCCL lacks distinctive imaging features, a multimodal imaging approach can enhance diagnostic accuracy (10). Ultrasound is typically used as an initial screening tool, where PSCCL often appears as an inhomogeneous hypoechoic mass within the liver, with a potential for extensive necrosis or cystic degeneration (1,6).

Table I. Temporal changes in tumor marker levels surrounding surgical intervention.

Time of examination	α-fetoprotein, μg/l	Carcinoembryonic antigen, μg/l	Carbohydrate antigen 19-9, KIU/l
Preoperative	2.4	11.6	228
7 days postoperative	3	4.6	44.1
40 days postoperative	3.8	3.7	10.8
90 days postoperative	1.9	12.8	321
100 days postoperative	2	12.6	440

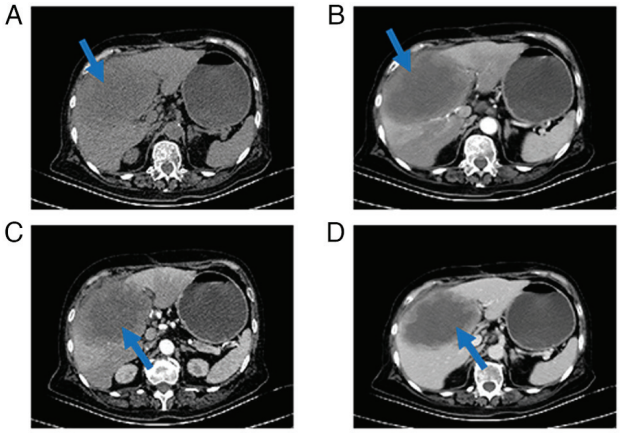

Figure 4. CT scan images of the patient, 100 days post-surgery. (A) Right lobe of the liver showed a slightly low-density shadow and an unclear edge of the lesion in the surgical area (blue arrow). (B) In the arterial phase, significant enhancement can be observed in the lesion (blue arrow), while there are focal and patchy areas of obvious enhancement at the periphery of the lesion. No enhancement is observed in the central low-density area of the lesion. (C) The details of arterial phase thin-layer lesions (blue arrow) are displayed more clearly. (D) In the portal venous phase, evident enhancement can still be observed in the lesion (blue arrow), and the solid enhancing component at the periphery of the lesion shows an increased range compared with the arterial phase, but no enhancement was found in the central low-density area.

CT scans, one of the primary diagnostic tools for PSCCL, usually reveal iso- or hypodense, solitary or multiple masses with indistinct margins and without a complete capsule (7). Larger tumors frequently exhibit extensive low-density necrotic areas (7,8). In contrast-enhanced CT scans, there is typically no significant enhancement during the arterial phase, although the tumor margins may show high-density rim enhancement; in the venous phase, the tumor edges usually appear isodense and may be associated with gallstones and liver cysts (8,10). CT can occasionally demonstrate tumor invasion into surrounding tissues or bile ducts, further supporting the diagnosis of PSCCL (4). In MRI, PSCCL typically presents as low signal intensity on T1-weighted imaging and high signal intensity on T2-weighted imaging, with diffusion-weighted imaging showing restricted diffusion (11). Early enhancement is usually weak, with peripheral nodular enhancement observed during the delayed phase (3,11). MRI is particularly valuable in delineating the extent of tumor infiltration and vascular involvement, which is crucial for surgical planning (3,11). PET-CT often reveals significant FDG uptake in PSCCL, indicating its highly invasive and malignant potential (9). Although literature on the PET-CT findings of PSCCL is limited, this imaging modality plays an important role in tumor staging and the assessment of systemic metastasis (8,9). In summary, while the imaging characteristics of PSCCL are not specific, the use of multiple imaging techniques can improve diagnostic accuracy. Ultrasound serves as an initial screening tool, while CT and MRI are pivotal in assessing the characteristics of the lesion and the staging of the tumor, with PET-CT demonstrating advantages in evaluating systemic metastasis. Further imaging studies may provide deeper insights into the imaging features of PSCCL and their diagnostic value.

Differential diagnosis. PSCCL needs to be differentially diagnosed from the following conditions:

1. Cholangiocarcinoma: Cholangiocarcinoma typically exhibits an infiltrative growth pattern with indistinct borders from the surrounding liver parenchyma and is often associated with bile duct dilatation (9). Enhanced CT or MRI usually demonstrates delayed enhancement, which is characteristic of this malignancy (9,15). Squamous cell carcinoma antigen testing may assist in differentiation (3).

2. Hepatocellular carcinoma (HCC): In liver contrast-enhanced imaging, HCC usually shows marked arterial phase enhancement ~35-45 sec after contrast injection, which is key for diagnosis (16). The late arterial phase is preferred for diagnosing and staging HCC, with rapid 'washout' observed during the portal venous and delayed phases (17). In the present case, MRI arterial phase scanning was performed ~35 sec after contrast injection, aligning with the traditional late arterial phase timing.

3. Hepatic cyst: When PSCCL exhibits significant necrosis, its imaging characteristics may resemble those of hepatic cysts, although important differences exist (18). Simple hepatic cysts appear as well-defined, non-enhancing low-density or low-signal areas on imaging, whereas PSCCL typically presents with thicker, irregular walls and shows enhancement on contrast studies, along with heterogeneous signals on MRI and prominent necrotic regions (19). Malignant transformation of hepatic cysts may show thickened walls, internal nodules or septations, typically displaying a more complex internal structure, while PSCCL tends to appear as a solid mass (8,18,19).

4. Metastatic tumors: Metastatic liver tumors usually present as single or multiple hypodense nodules with ring enhancement, often accompanied by a history of malignancy in other organs (20). Common imaging signs include the 'target sign' and 'bull's-eye sign', and PET-CT can be helpful in identifying the primary tumor (21).

5. Liver abscess: On CT scanning, a liver abscess appears as a round hypodense lesion with enhanced walls during contrast scans, while the surrounding edema remains non-enhancing, forming a ring sign (22). It is usually associated with fever and elevated white blood cell counts (9,22).

Treatments and prognosis. PSCCL is an exceedingly rare and highly aggressive hepatic malignancy (1-11). Due to its rarity, treatment strategies are primarily based on case reports and small case series (1-11). Common treatment modalities include surgical resection, chemotherapy, radiotherapy and transcatheter arterial chemoembolization (TACE) (2,4-8). However, the efficacy of these approaches remains uncertain due to the aggressive nature and high recurrence rate of PSCCL (2,5,7). Surgical resection is generally considered one of the most effective treatments for PSCCL (4,8,23). Studies by Iimuro *et al* (6) and Zhao *et al* (1) indicate that early surgical intervention before tumor spread into the surrounding hepatic parenchyma is closely associated with improved prognosis. Weimann *et al* (19) reported a case of long-term survival following surgery alone, with the patient surviving over four years without adjuvant chemotherapy or radiotherapy. This outcome suggests that early and complete tumor resection may prolong survival. The systematic review by Zhao *et al* (1) also states that chemotherapy and radiotherapy are commonly employed for patients with PSCCL post-surgery or those who are inoperable, aiming to control tumor progression. Boscolo *et al* (24) reported successful treatment of advanced primary SCC with systemic therapy using CDDP and 5-FU along with surgical resection. Although these treatments are standard in oncology, and their efficacy in PSCCL has not been well-established (1,4,6).

The prognosis for PSCCL is generally poor. Although early surgical intervention may extend survival, the majority of cases eventually recur (5,7,8). Zhang *et al* (8) indicated that patients who undergo curative surgery have significantly longer overall survival than those receiving palliative treatment (8). However, the high recurrence rate remains a major challenge even after curative resection (5,7,8). Rezvani *et al* (25) reported on a case of recurrence six weeks after radical surgery. No reoperation or chemotherapy was performed, and after five months of palliative care, the patient succumbed to the disease. Weimann *et al* (19) also found that despite some patients achieving prolonged survival without adjuvant therapy, most still face the risk of recurrence post-surgery (19). Further research and the accumulation of more cases are essential to explore more effective treatment options to improve patient quality of life and prognosis.

In summary, PSCCL is an extremely rare and highly aggressive hepatic malignancy, characterized by non-specific clinical and imaging features, making diagnosis and treatment challenging. The pathogenesis of this tumor may be associated with factors such as chronic liver disease and inflammatory responses. Due to the difficulty in early diagnosis, comprehensive evaluation typically requires multimodal imaging techniques. Although early surgical resection is considered the primary treatment approach, the high recurrence rate significantly impacts prognosis. To improve the diagnostic accuracy and treatment outcomes for PSCCL, future research should focus on several key areas including deeper exploration of its pathogenesis, the development of more advanced multimodal imaging techniques, optimization of personalized treatment strategies and enhanced sharing of global case data. These efforts hold the potential to extend patient survival and improve quality of life. Additionally, tumor markers such as CEA and CA19-9 may provide valuable insights for diagnosis and prognostic assessment. Increasing awareness and understanding of this rare malignancy are crucial for early detection, accurate diagnosis and effective treatment.

Acknowledgements

Not applicable.

Funding

No funding was received.

Availability of data and materials

The data generated in the present study may be requested from the corresponding author.

Authors' contributions

GS and XM designed the study and participated in the literature search. GS obtained the medical images, contributed to the literature review and prepared the draft manuscript. XY, FY and ZW revised the manuscript, participated in data analysis and provided treatment recommendations for the patient. XM and GS confirm the authenticity of all the raw data. All authors read and approved the final version of the manuscript.

Ethics approval and consent to participate

The present study included no personal information disclosure, and was approved by The Ethics Committee of Zhuji People's Hospital [Zhuji, China; approval no. (2024); MedEthics no. (0506)].

Patient consent for publication

Written informed consent was provided by the patient to obtain clinical data and information, as well as for publication.

Competing interests

The authors declare that they have no competing interests.

References

1. Zhao L, Zhou Y, Ding J, Qin Z, Zhou H and Jing X: Primary hepatic squamous cell carcinoma: Case report and systematic review of the literature. Front. Oncol 13: 1229936, 2023.
2. Benhamdane A, Adioui T, Berrag S, Nejjari F, Allaoui M and Tamzaourte M: Primary squamous cell carcinoma of the liver. Eur J Case Rep Intern Med 11: 004628, 2024.
3. Fakhreddine O, Fadlallah Y, Turfa J, Hassan MA, Chamseddine N and Assi HI: Primary squamous cell carcinoma of the liver: Case report and review of literature. Case Rep Oncol 15: 480-485, 2022.
4. Lee HL, Liu YY, Yeh CN, Chiang KC, Chen TC and Jan YY: Primary squamous cell carcinoma of the liver: A successful surgically treated case. World J Gastroenterol 12: 5419-5421, 2006.

5. Lyagoubi M, Mehdaoui C, Haloui A, Karish N, Ismaili Z and Bennani A: Primary hepatic squamous cell carcinoma: A case report. Cureus 16: e63803, 2024.
6. Iimuro Y, Asano Y, Suzumura K, Yada A, Hirano T, Iijima H, Nishiguchi S, Hirota S and Fujimoto J: Primary squamous cell carcinoma of the liver: An uncommon finding in contrast-enhanced ultrasonography imaging. Case Rep Gastroenterol 5: 628-635, 2011.
7. Xiao J, Ma L, Li J, Yin B, Liang J and Wang J: Primary squamous cell carcinoma of the liver is rare but hostile: Case series and comprehensive review of the literature. Cancer Manag Res 13: 829-837, 2021.
8. Zhang XF, Du ZQ, Liu XM and Lv Y: Primary squamous cell carcinoma of liver: Case series and review of literatures. Medicine (Baltimore) 94: e868, 2015.
9. Sun Y and Jin G: Primary squamous cell carcinoma of the liver: A case report. J Int Med Res 49: 3000605211021275, 2021.
10. Song Y, Shi J, Zhang X, Qiao M, Sun Z and Tian S: Diagnostic value of imaging modalities in primary squamous cell carcinoma of the liver. J Clin Ultrasound 51: 887-897, 2023.
11. Atiq M, Ammar AS, Ali RM, Haider S, Ahmed I and Dar FS: Primary squamous cell carcinoma of liver. First case report from Pakistan and South Asia. Int J Surg Case Rep 99: 107655, 2022.
12. Valenti L, Pelusi S, Bianco C, Ceriotti F, Berzuini A, Iogna Prat L, Trotti R, Malvestiti F, D'Ambrosio R, Lampertico P, *et al*: Definition of healthy ranges for alanine aminotransferase levels: A 2021 update. Hepatol Commun 5: 1824-1832, 2021.
13. Zhang Y, Abdollahi A, Andolino C, Tomoo K, Foster BM, Aryal UK and Henderson GC: Performance evaluation of different albumin assays for the detection of analbuminemia. PLoS One 19: e0300130, 2024.
14. Llovet JM, Kelley RK, Villanueva A, Singal AG, Pikarsky E, Roayaie S, Lencioni R, Koike K, Zucman-Rossi J and Finn RS: Hepatocellular carcinoma. Nat Rev Dis Primers 7: 6, 2021.
15. Viganò L and Fiz F: ASO author reflections: Radiomics for intrahepatic cholangiocarcinoma: A further step toward precision surgery. Ann Surg Oncol 31: 5647-5648, 2024.
16. Kim YY, Lee S, Shin J, Son WJ, Roh YH, Hwang JA and Lee JE: Diagnostic performance of CT versus MRI liver imaging reporting and data system category 5 for hepatocellular carcinoma: A systematic review and meta-analysis of comparative studies. Eur Radiol 32: 6723-6729, 2022.
17. Zhao C, Dai H, Shao J, He Q, Su W, Wang P, Tang Q, Zeng J, Xu S, Zhao J and Xiang S: Accuracy of various forms of contrast-enhanced MRI for diagnosing hepatocellular carcinoma: A systematic review and meta-analysis. Front Oncol 11: 680691, 2021.
18. Armutlu A, Quigley B, Choi H, Basturk O, Akkas G, Pehlivanoglu B, Memis B, Jang KT, Erkan M, Erkan B, *et al*: Hepatic cysts: Reappraisal of the classification, terminology, differential diagnosis, and clinicopathologic characteristics in 258 Cases. Am J Surg Pathol 46: 1219-1233, 2022.
19. Weimann A, Klempnauer J, Gebel M, Maschek H, Bartels M, Ringe B and Pichlmayr R: Squamous cell carcinoma of the liver originating from a solitary non-parasitic cyst case report and review of the literature. HPB Surg 10: 45-49, 1996.
20. Berlin JW, Gore RM, Yaghmai V, Pereles FS and Miller FH: Radiologic imaging and staging of primary and metastatic liver tumors. Cancer Treat Res 109: 39-58, 2001.
21. Fukumoto W, Nakamura Y, Higaki T, Tatsugami F, Iida M and Awai K: Additional value of diffusion-weighted MRI to Gd-EOB-DTPA-enhanced Hepatic MRI for the detection of liver metastasis: The difference depending on the experience of the radiologists. Hiroshima J Med Sci 64: 15-21, 2015.
22. Sutherland T, Temple F, Lee WK and Hennessy O: Evaluation of focal hepatic lesions with ultrasound contrast agents. J Clin Ultrasound 39: 399-407, 2011.
23. Okuda Y, Abe T, Ikeda M, Kurihara K, Shimizu A, Oshita A, Yonehara S and Hanada K: Curative surgery for primary squamous cell carcinoma of the liver: A rare case study. Clin J Gastroenterol 16: 263-269, 2023.
24. Boscolo G, Jirillo A and Da Pian P: Complete remission of poorly differentiated squamous liver carcinoma after systemic chemotherapy and surgery. A case report. Tumori 91: 71-72, 2005.
25. Rezvani H, Azhdari Tehrani H, Salari S, Feiziazar S and Darnahal M: Primary squamous cell carcinoma of the liver: A case report. Gastroenterol Hepatol Bed Bench 15: 430-434, 2022.